Advances in fluorescent protein technology

Nathan C. Shaner[1], George H. Patterson[2] and Michael W. Davidson[3]

[1]The Salk Institute for Biological Studies, 10010 North Torrey Pines Road, La Jolla, CA 92037, USA
[2]Cell Biology and Metabolism Branch, National Institute of Child Health and Human Development (NICHD), Bethesda, MD 20892, USA
[3]National High Magnetic Field Laboratory and Department of Biological Science, The Florida State University, Tallahassee, FL 32310, USA
e-mails: shaner@salk.edu; pattersg@mail.nih.gov; davidson@magnet.fsu.edu

Summary

Current fluorescent protein (FP) development strategies are focused on fine-tuning the photophysical properties of blue to yellow variants derived from the *Aequorea victoria* jellyfish green fluorescent protein (GFP) and on the development of monomeric FPs from other organisms that emit in the yellow-orange to far-red regions of the visible light spectrum. Progress toward these goals has been substantial, and near-infrared emitting FPs may loom over the horizon. The latest efforts in jellyfish variants have resulted in new and improved monomeric BFP, CFP, GFP and YFP variants, and the relentless search for a bright, monomeric and fast-maturing red FP has yielded a host of excellent candidates, although none is yet optimal for all applications. Meanwhile, photoactivatable FPs are emerging as a powerful class of probes for intracellular dynamics and, unexpectedly, as useful tools for the development of superresolution microscopy applications.

Key words: Fluorescent proteins, Mutagenesis, Optical highlighters, Photoactivation, Photoconversion, Photoswitching, Live-cell imaging

Introduction

The rapid rise of fluorescent proteins (FPs) as a fundamental staple of biomedical research has often been termed a revolution, the first phase of which began just over a decade ago when the original *Aequorea victoria* jellyfish wild-type green fluorescent protein (GFP) was elegantly used to highlight sensory neurons in the nematode (Chalfie et al., 1994). Since then, the race has been on to produce new and improved versions that are brighter, cover a broad spectral range, and also exhibit enhanced photostability, reduced oligomerization, pH insensitivity, and faster maturation rates. The wild type (wtGFP) was quickly modified to produce variants emitting in the blue (BFP), cyan (CFP) and yellow (YFP) regions (Fig. 1) (Heim et al., 1994; Ormö et al., 1996; Tsien, 1998), but the orange and red spectral regions have remained unachievable with *Aequorea* GFP and were surprisingly elusive until the unexpected discovery of the first red FP from a non-bioluminescent reef coral (Matz et al., 1999). This breakthrough launched a second phase of the revolution, the relentless quest for the holy grail of fluorescent proteins, a bright and photostable monomeric red-emitting derivative, whose performance matches that of the best GFP variants. The search continues on today. So far, progress has generally been very encouraging, although there still remains a significant performance gap in many FP spectral classes.

Despite the recent advances in FP technology, most groups still use the enhanced version of wild-type GFP (EGFP), as well as the original cyan and yellow derivatives (ECFP and EYFP), for the majority of their imaging applications (Olenych et al., 2006; Patterson, 2007). The reluctance of many researchers to transition to newer FP variants is fueled by the checkered availability of various FPs, coupled with (often justified) uncertainties about reported claims of improved brightness, photostability, monomeric character and utility in fusions. In many cases, simply finding a source for a new FP can be a time-consuming and discouraging challenge. The lack of dependable commercial sources often requires researchers to rely on the generosity of the original laboratory, which in turn can be bombarded with an avalanche of requests shortly after a new protein or fusion construct has been reported. Barring the implementation of an organized and efficient system for the distribution of FP variants to the scientific community, this situation is unlikely to improve in the near future.

Here, we attempt to address frequent misconceptions that occur during the transition to new FP variants, including the issue of oligomerization. In addition, we discuss recent advances in protein engineering strategies as well as improvements to the color palette and the development of the current armament of photoactivatable FPs. Finally, we provide suggestions for the best FP choices in single- and multi-color imaging, and potential avenues for obtaining these proteins.

New additions to the FP color palette

The broad range of FP genetic variants developed over the past several years feature fluorescence emission profiles spanning almost the entire visible light spectrum (Chudakov et al., 2005; Shaner et al., 2005; Verkhusha and Lukyanov, 2004). Several guiding motifs have emerged regarding the fundamental origins and manipulation of the emission color (Remington, 2006). Local environmental variables around the chromophore, including the position of charged amino acid residues, hydrogen bonding networks and hydrophobic interactions within the protein matrix, can produce blue or red spectral shifts in the absorption and emission maxima of as much as 40 nm. Larger spectral shifts, which distinguish the general FP spectral class (CFP, GFP, YFP, etc.), are generally attributed to differences in the covalent structure and the extent of π-orbital
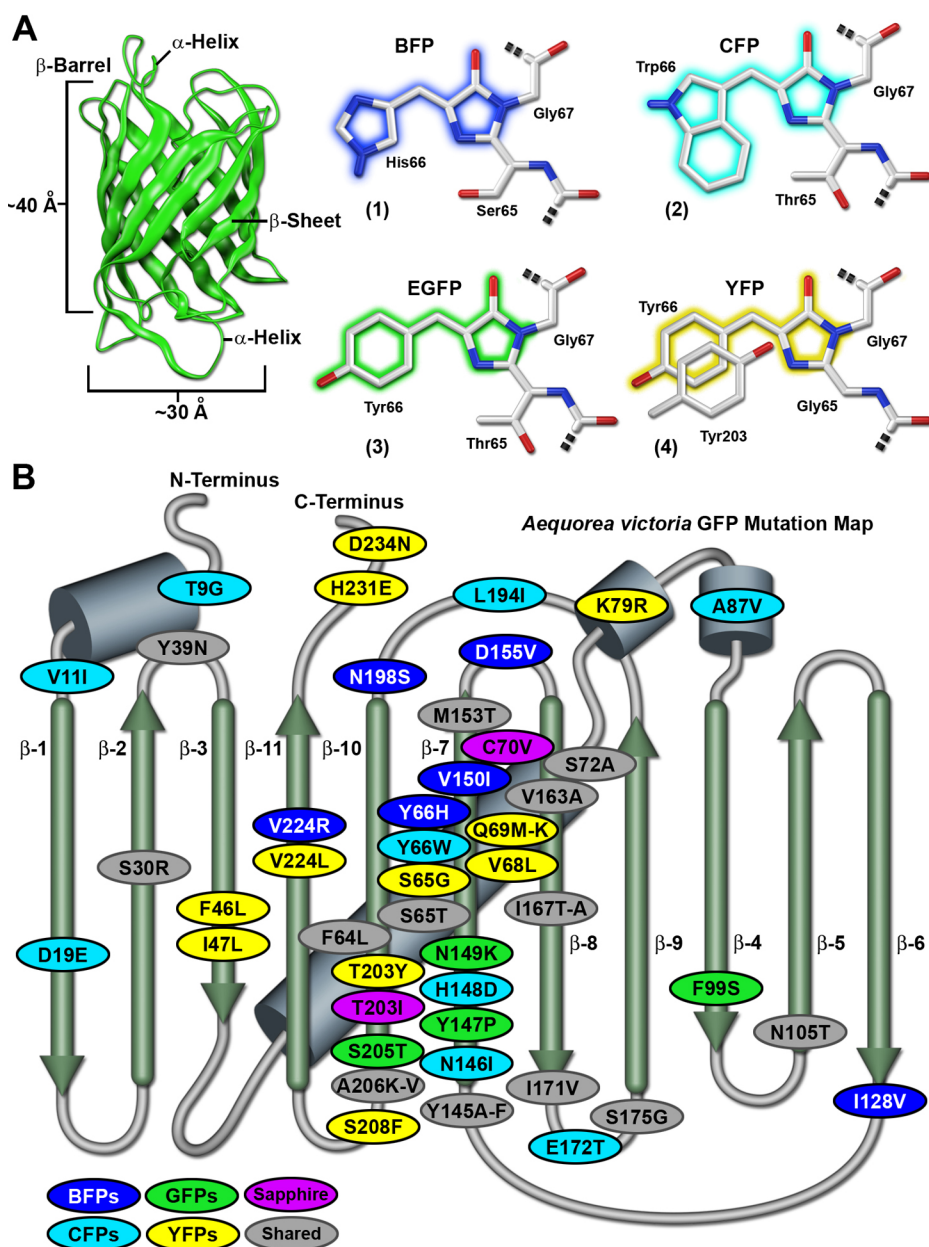
Fig. 1. (A) FP β-barrel architecture and approximate dimensions, and chromophore structures of common *Aequorea* FP derivatives. (1) BFP, (2) CFP, (3) EGFP, (4) YFP. The tryptophan residue (Trp66) in (2) is illustrated in the cis conformation as occurs for Cerulean derivatives (Malo et al., 2007) rather than the trans isomer that is common to CFP and related variants. Portions of the chromophores that are conjugated and give rise to fluorescence are shaded with colors corresponding to the emission spectral profile. (B) *Aequorea* GFP mutation map showing common mutations superimposed on a topological layout of the peptide structure. β-sheets are numbered and depicted as thin, green cylinders with an arrow pointing towards the C-terminus, whereas α-helices are depicted as gray cylinders. Mutations are color-coded to represent the variants to which they apply: BFPs (blue), CFPs (cyan), GFPs (green), YFPs (yellow), Sapphire (violet), folding, shared and monomerizing (gray). Note that almost 75% of the mutations are located in the central helix and in β-sheet strands 7, 8 and 10. In general, wavelength-specific mutations occur near the central helix containing the chromophore, whereas folding mutations occur throughout the sequence. Many of the cyan and yellow FP mutations introduced near the termini of the proteins resulted during the CyPet and YPet mutagenesis efforts (Nguyen and Daugherty, 2005). Several of the sfGFP folding mutations (S30R, Y39N, F99S and N105T) also occur away from the chromophore. The monomerizing mutation A206K is useful for all known GFP derivatives, but is replaced by A206V in sfGFP and EBFP2.

conjugation of the chromophore (Figs 1 and 2). As further studies into the complex characteristics of FP chromophores yield clues about the structure-function relationship with the polypeptide backbone, the task of genetically engineering more finely tuned color variants and broadening the spectral range of useful proteins should become easier.

Blue and cyan FPs

Although most attention now focuses on the orange-to-far-red spectral regions, recent BFP and CFP variants have dramatically strengthened the potential for imaging in these regions as well. Although EBFP was one of the first spectral variants derived from *Aequorea* GFP, its low brightness and poor photostability have long made it an unattractive option for most researchers. Three groups (Ai et al., 2007; Kremers et al., 2007; Mena et al., 2006) have recently reported improved blue *Aequorea* FP variants that feature significantly higher brightness and photostability compared with EBFP. Named Azurite, SBFP2 (strongly enhanced blue fluorescent protein) and EBFP2 (Fig. 3A), these novel variants offer the first real hope for successful long-term imaging of live cells in the blue spectral region. Even though all three probably exhibit weakly dimeric character in highly concentrated microenvironments (Zacharias et al., 2002), they function effectively in fusions with subcellular localization targeting proteins (Ai et al., 2007; Kremers et al., 2007) (M.W.D., unpublished) and can be readily imaged with standard BFP and 4′,6-diamidino-2-phenylindole (DAPI) filter sets. All of these new BFP variants could potentially be made truly monomeric by addition of the A206K mutation, which is unlikely to have any substantial negative impact on their properties. Furthermore, EBFP2, the brightest and most photostable blue FP (see Table 1), is an excellent fluorescence resonance energy transfer (FRET) donor (M.W.D., unpublished) for EGFP in live cells.
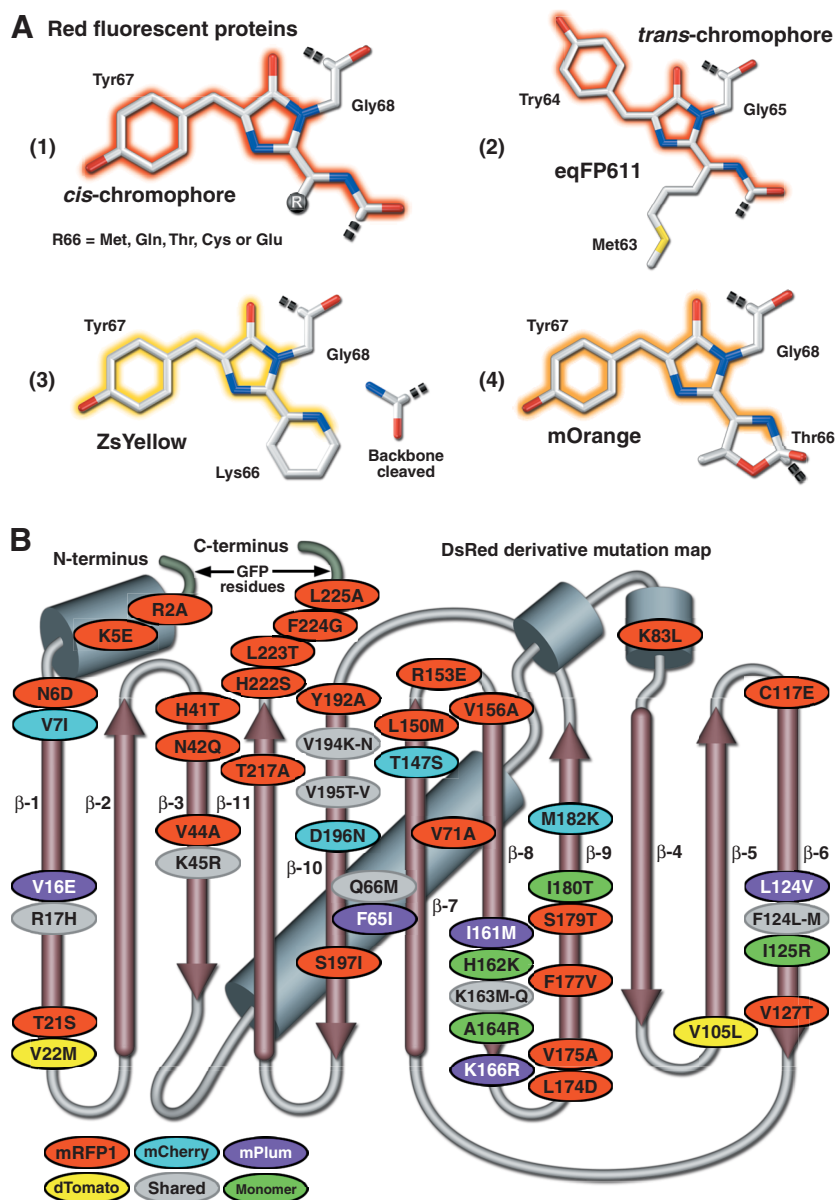
Fig. 2. (A) Chromophore structural variation in yellow, orange, and red FPs. (1) FPs derived from DsRed and other reef coral organisms thought to have a cis-chromophore. The residue at position 66 can be Met, Gln, Thr, Cys or Glu. (2) eqFP611, a red variant derived from *Entacmaea quadricolor*, is the only known FP featuring a trans-chromophore (Petersen et al., 2003). (3) ZsYellow (also zFP538), derived from the button polyp *Zoanthus*, features a novel three-ring chromophore that is created when the lysine residue at position 66 cyclizes with its own α-carbon to form a tetrahydropyridine ring conjugated to the chromophore (Remington et al., 2005). (4) mOrange, one of the mFruit proteins (Shaner et al., 2004), also features a three-ring chromophore where Thr66 cyclizes with the preceding carbonyl carbon to yield a partially conjugated oxazole ring (Shu et al., 2006). (B) DsRed mutation map showing mutations of useful variants superimposed on a topological layout of the peptide structure. β-sheets are numbered and depicted as thin, red cylinders with an arrow pointing towards the C-terminus, whereas α-helices are depicted by gray cylinders. Extensions of the N- and C-termini due to the addition of amino acids derived from GFP to improve fusion performance are shaded in light green. Mutations are color-coded to represent the variants to which they apply: mRFP1 (red), mCherry (cyan), mPlum (violet), dTomato (yellow), monomerizing mutations (green) and shared mutations (gray). Note that unlike the cluster of mutations surrounding the chromophore for *Aequorea* GFP variants (Fig. 1), red FP mutations are distributed throughout the sequence.

The cyan spectral region (~470 nm to 500 nm) was dominated by progeny of the original *Aequorea* ECFP (Table 1) until the introduction of a monomeric teal-colored variant, mTFP1 (Fig. 3C; Allele Biotech), that has even higher brightness levels, acid insensitivity and greater photostability (Ai et al., 2006). Derived from a tetrameric *Clavularia* soft coral protein, mTFP1 has spectral characteristics that are slightly red-shifted with respect to most CFPs (thus the name teal rather than cyan). Unlike other CFPs, which generally feature the heteroaromatic amino acid tryptophan at position 66 in the chromophore, mTFP1 contains a tyrosine residue at this location. Substituting tyrosine for tryptophan reduces the broad fluorescence emission spectral width from ~60 nm to a narrower and more manageable 30 nm, which reduces bleed-through in multicolor and FRET experiments. The high quantum yield of mTFP1 (see Table 1) provides an excellent alternative to the cyan derivatives mECFP (Shaner et al., 2005) and mCerulean (Fig. 3B) (Rizzo et al., 2004) as a FRET donor when combined with either yellow or orange FPs. On the downside, mTFP1 requires a specialized filter set for optimal imaging, but it can still produce suitable signal levels with a standard ECFP filter set.

Recently, a comprehensive site-directed mutagenesis approach has been applied to optimize previously identified mutations in monomeric variants of ECFP and EYFP (Fig. 1) for enhanced brightness, folding efficiency, solubility and FRET performance (Kremers et al., 2006). The resulting super cyan and yellow fluorescent derivatives, termed SCFP and SYFP, are significantly brighter than the parent proteins when expressed in bacteria, but less than twofold brighter in mammalian cells. Nevertheless, these high-performance FPs should be useful for fusion tags and for creating new, advanced CFP-YFP FRET biosensors exhibiting high dynamic range for the detection of metabolites, pH changes, Ca^{2+} fluctuations, protein and enzyme phosphorylation, as well as a host of other intracellular processes.

Table 1. Physical properties of useful fluorescent proteins

Protein*	Color of spectral class	Excitation peak (nm)	Emission peak (nm)	Brightness[†]	Photostability[‡]	pKa[‡]	Association state[‡]	Chromophore	Filter set[§]	Reference
EBFP2	Blue	383	448	18	55	5.3	Weak dimer	SHG	DAPI/BFP	Ai et al., 2007
ECFP[‡‡]	Cyan	433/445	475/503	13	64	4.7	Weak dimer	TWG	CFP	Cubitt et al., 1995
mCerulean	Cyan	433/445	475/503	27/24	36	4.7	Monomer	TWG	CFP	Rizzo et al., 2004
mTFP1	Cyan-green	462	492	54	110	4.3	Monomer	AYG	CFP	Ai et al., 2006
mEGFP	Green	488	507	34	174	6.0	Monomer	TYG	FITC/GFP	Heim et al., 1995
mEmerald	Green	487	509	39	101[¶]	6.0	Monomer	TYG	FITC/GFP	Cubitt et al., 1999
sfGFP	Green	485	510	54	157[¶]	5.5	Weak dimer	TYG	FITC/GFP	Pédelacq et al., 2006
EYFP[‡‡]	Yellow	514	527	51	60	6.9	Weak dimer	GYG	FITF/YFP	Miyawaki et al., 1999
mVenus	Yellow	515	528	53	15	6.0	Monomer	GYG	FITC/YFP	Nagai et al., 2002
mCitrine	Yellow	516	529	59	49	5.7	Monomer	GYG	FITC/YFP	Griesbeck et al., 2001
YPet	Yellow	517	530	80	49	5.6	Weak dimer	GYG	FITC/YFP	Nguyen and Daugherty, 2005
mKO	Orange	548	559	31	122	5.0	Monomer	CYG	TRITC/DsRed	Karasawa et al., 2004
tdTomato	Orange	554	581	95	98	4.7	T-dimer	MYG	TRITC/DsRed	Shaner et al., 2004
TagRFP	Orange	555	584	48	37**	<4.0	Monomer	MYG	TRITC/DsRed	Merzlyak et al., 2007
mRFP1[‡‡]	Red	584	607	12.5	8.7	4.5	Monomer	QYG	TxRed	Campbell et al., 2002
mCherry	Red	587	610	17[††]	96	<4.5	Monomer	MYG	TxRed	Shaner et al., 2004
mKate	Far-red	588	635	15	166[¶]	6.0	Monomer	MYG	TxRed	Shcherbo et al., 2007
mPlum	Far-red	590	649	3.2[††]	53	<4.5	Monomer	MYG	TxRed	Wang et al., 2004

Physical properties for the recommended FPs in each spectral class. *Common literature FPs in each spectral class. *Common literature FP abbreviation. [†]Product of the molar extinction coefficient and the quantum yield (mM×cm)[-1]. [‡]Literature values except as noted. Photobleaching represents the time to bleach from an emission rate of 1000 photons per second to 500 photons per second (t[1/2]) in a widefield fluorescence microscope. [§]Recommended common filter sets and custom FP sets available from aftermarket manufacturers. For specialized applications, we suggest choosing filter combinations that closely match the spectral profiles (see Shaner et al., 2005). [¶]Measured in live cells with mEGFP (t[1/2]=150 seconds) as a control. **Measured and normalized per standard photobleaching protocol (see Shaner et al., 2005). [††]Averages of literature values. [‡‡]Included for reference.

Green FPs

Numerous proteins emitting in the green (500 nm to 525 nm) spectral region have been discovered from a wide range of sources, including different *Aequorea* species (Labas et al., 2002), copepods (Shagin et al., 2004), amphioxus (Deheyn et al., 2007) and reef corals (Matz et al., 1999). Most, however, exhibit oligomerization artifacts, and even the best offer no clear advantage over EGFP (Table 1; Fig. 3M-Q). Perhaps the best current choice for live-cell imaging is the GFP derivative Emerald (Fig. 3D; Invitrogen), which has similar properties to those of its EGFP parent (Cubitt et al., 1999). Emerald contains the F64L and S65T mutations featured in EGFP, but also has four additional point mutations that improve folding, mutation rate at 37°C and brightness. Although Emerald is somewhat more efficient than EGFP, it has a fast photobleaching component that might affect quantitative imaging in some environments [this artifact is likely to be reduced in monomeric A206K variants (N.C.S., unpublished)]. The most significant addition to the GFP palette in the past several years is superfolder GFP (Fig. 3E) (Pédelacq et al., 2006), which can efficiently fold even when fused to insoluble proteins and is slightly brighter and more acid resistant than either EGFP or Emerald (Table 1). Note, however, that superfolder GFP may generate higher background noise levels when one images fusions in which a significant number of the proteins fail to target correctly but still produce bright fluorescence.

Yellow FPs

Yellow FPs, as a spectral class, are among the brightest and most versatile genetically encoded probes yet developed. However, the original variant, EYFP (Table 1), although still widely used, is far from optimal owing to its high pK_a and sensitivity to halides. The monomeric YFP variants mCitrine and mVenus (Fig. 3F) are currently the most useful probes in the yellow class (see Table 1), but neither is commercially available. However, a similar but less well characterized *Aequorea* derivative, named after the birthstone Topaz (Cubitt et al., 1999), can be purchased from Invitrogen. In addition, the newly developed SYFP (discussed above) should become a useful member of the yellow palette once its performance in fusions expressed in mammalian cells is confirmed.

Another potentially useful YFP, YPet (**y**ellow fluorescent **p**rotein for **e**nergy **t**ransfer), was derived from synthetic DNA shuffling coupled with fluorescence-activated cell sorting (FACS) to enhance the pairing of cyan and yellow proteins for FRET (Nguyen and Daugherty, 2005). YPet is the brightest YFP variant yet developed and demonstrates very good photostability (Fig. 3G; Table 1). The resistance to acidic environments afforded by YPet is superior to Venus and other YFP derivatives, which will enhance the utility of this probe in biosensor combinations targeted at acidic organelles. Although optimized for FRET, there remains a serious doubt as to the origin of YPet's increased performance, which is likely to be due simply to enhanced dimerization with its co-evolved partner CyPet (Ohashi et al., 2007; Vinkenborg et al., 2007).

Orange FPs

In contrast to the hundreds of FPs engineered in the cyan, green and yellow spectral classes, only few probes have been developed so far that emit in the orange and red wavelengths (~560 nm to 650 nm). Even so, the existing proteins in these spectral classes (see Fig. 2 and Table 1), which have all been isolated from coral species, exhibit the potential to be useful in a variety of imaging scenarios. A point of confusion exists in the nomenclature for FPs in the orange region. Often termed red fluorescent proteins (RFPs – perhaps wishful thinking on the part of the discoverers), probes such as DsRed, TagRFP, and tdTomato (Matz et al., 1999; Merzlyak et al., 2007; Shaner et al., 2004) actually have emission profiles that are clearly more orange than red. Regardless of the color designation, proteins in the orange spectral class are readily imaged in multicolor scenarios, using a standard tetramethyl-rhodamine isothiocyanate (TRITC) filter set, when coupled with cyan, green and red FPs.

Kusabira Orange was originally derived as a tetramer from the mushroom coral *Fungia concinna* through site-specific mutagenesis of a cDNA clone in which ten residues were added to the N-terminus of the protein (Karasawa et al., 2004). The resulting FP has an absorption maximum at 548 nm and emits bright yellow-orange fluorescence centered at 559 nm. A monomeric version (mKO; Fig. 3H) was subsequently created by introduction of an additional 20 mutations. mKO exhibits a brightness value similar to that of EGFP and its photostability in widefield-fluorescence illumination is among the best of any FP, which makes it an excellent choice for long-term imaging experiments (see Table 1). Furthermore, the high extinction coefficient should render mKO an excellent FRET acceptor for cyan and teal FPs. Both the tetrameric and monomeric variants of Kusabira Orange are now commercially available (from MBL International).

A bright new monomeric orange protein, TagRFP, has recently been introduced as a promising candidate for localization and FRET studies (Merzlyak et al., 2007). Originally cloned as a dimer from the sea anemone *Entacmaea quadricolor*, subsequent random mutagenesis yielded a rapidly maturing variant, TurboRFP (commercially available from Evrogen), featuring high photostability, brightness and pH resistance. On the basis of the crystal structure of a closely related protein from the same species (eqFP611; Fig. 2), Merzlyak et al. replaced several key amino acid residues involved in dimerization, while simultaneously performing random mutagenesis to rescue the folding properties. The final variant, TagRFP (from Evrogen), has very favorable photophysical properties (Table 1) and performs well in a wide variety of fusions expressed in mammalian cells (M.W.D., unpublished) (Merzlyak et al., 2007) (Fig. 3J). However, its photostability in our hands is not as high as was originally claimed (Merzlyak et al., 2007; Shcherbo et al., 2007) (see Table 1). Merzlyak et al. speculate that TagRFP will be an excellent FRET acceptor when fused to GFP and YFP donors, but that remains to be demonstrated.

Several of the major problems with the original *Discosoma* DsRed FP (slow maturation, an intermediate green state, and the obligate tetrameric character) were overcome through site-directed and random mutagenesis efforts, but the construction of true monomeric DsRed variants, as well as monomers from proteins in other Anthozoa species, has proven to be a difficult task (Campbell et al., 2002; Rizzo and Piston, 2005; Verkhusha and Lukyanov, 2004). A total of 33 residue alterations to the DsRed sequence were required for the creation of the first-generation monomeric red FP (mRFP1) (Campbell et al., 2002), which has absorption and emission maxima at 584 nm
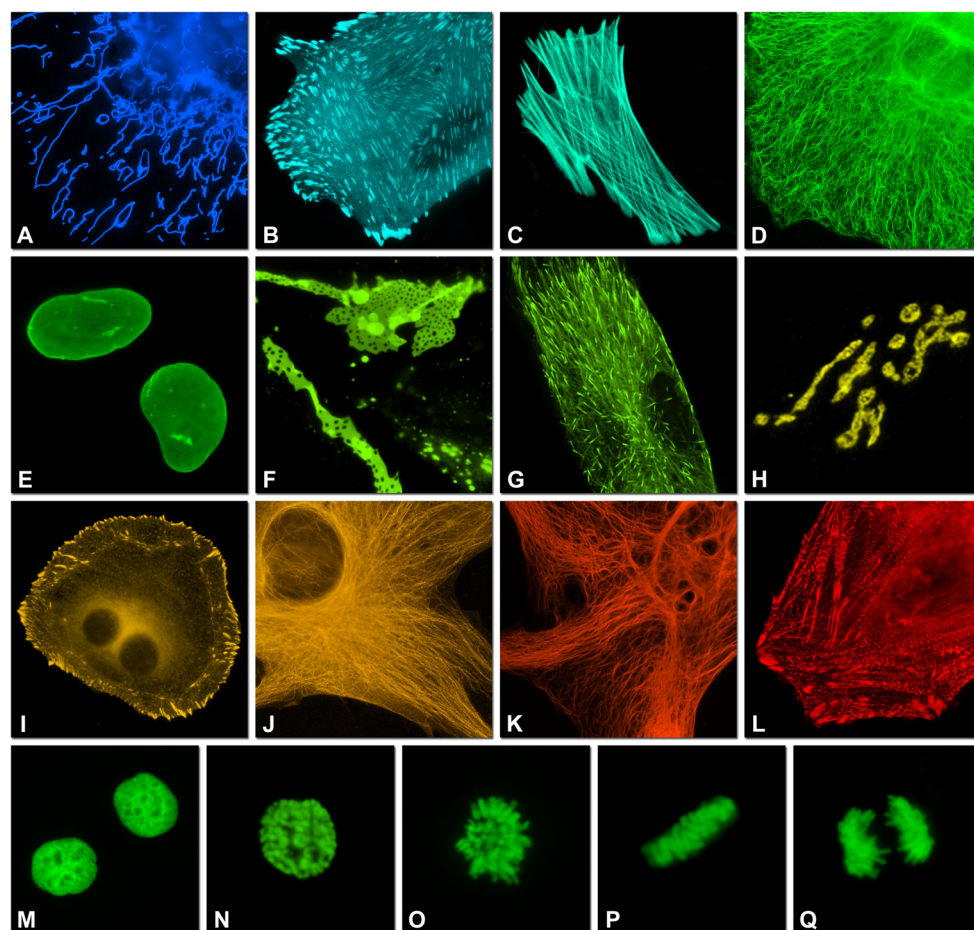
Fig. 3. (A-L) Subcellular localization of selected monomeric FP fusions (listed in Table 1) with targeting proteins imaged in widefield fluorescence. Images are pseudocolored to match the FP emission profile. The FP fusion terminus and number of linker amino acids is indicated after the name of the targeted organelle or fusion protein. (A) EBFP2-mito-N-7 (human cytochrome C oxidase subunit VIII; mitochondria); (B) mCerulean-paxillin-N-22 (chicken; focal adhesions); (C) mTFP1-actin-C-7 (human β-actin; filamentous actin); (D) mEmerald-keratin-N-17 (human cytokeratin 18; intermediate filaments); (E) superfolder GFP-lamin B1-C-10 (human lamin B1; nuclear envelope); (F) mVenus-Cx43-N-7 (rat α-1 connexin-43; gap junctions); (G) YPet-EB3-N-7 (human microtubule-associated protein; RP/EB family); (H) mKO-Golgi-N-7 (N-terminal 81 amino acids of human β-1,4-glactosyltransferase; Golgi complex); (I) tdTomato-zyxin-N-7 (human zyxin; focal adhesions); (J) TagRFP-tubulin-C-6 (human α-tubulin; microtubules); (K) mCherry-vimentin-N-7 (human vimentin; intermediate filaments); (L) mPlum-α-actinin-N-19 (human non-muscle; cytoskeleton). (M-Q) Fusion of mEGFP with human histone H2B (mEGFP-H2B-N-6). (M) interphase; (N) prophase; (O) prometaphase; (P) metaphase; (Q) anaphase.

and 607 nm, respectively. However, this derivative exhibits significantly reduced fluorescence emission compared with the native protein and photobleaches very quickly, rendering it much less useful than analogous monomeric GFPs and YFPs. Extensive mutagenesis efforts (discussed below), have successfully been applied in the search for orange, red and far-red FP variants that further reduce the tendency of these potentially advantageous biological probes to self-associate while simultaneously pushing emission maxima towards longer wavelengths

The brightest FP in any spectral class is the tandem version of dimeric (d) Tomato, an orange derivative that was one of the original 'Fruit' proteins (Shaner et al., 2004). dTomato was derived from an intermediate termed dimer2, generated during the breakup of the tetrameric DsRed protein (Campbell et al., 2002). This variant contains the first and last seven residues from GFP on its N- and C-termini, which is intended to increase tolerance to fusion proteins and reduce potential localization artifacts. A tandem-dimer version (effectively a monomer) contains two copies – head-to-tail – of dTomato with a 12-residue linker. Because of its twin chromophores, the resulting tdTomato (Fig. 3I) is extremely bright and, moreover, is also exceptionally photostable under widefield illumination (Table 1). The major drawback of tdTomato is its larger size, which may interfere with fusion-protein packing in some biopolymers.

Red FPs

The quest for a well-behaved red-emitting FP has long been the goal for live-cell and whole-animal imaging, primarily because of the requirement for red probes in multicolor imaging experiments, and the fact that longer excitation wavelengths generate less phototoxicity and can probe deeper into biological tissues. Perhaps the most dramatic development on this front has been the introduction of new FPs derived from mRFP1 through directed mutagenesis targeting chromophore residues that are known to play a key role in determining the spectral characteristics (Fig. 2) (Patterson, 2004; Shaner et al., 2004). The resulting monomeric FPs exhibit maxima at wavelengths from 560 nm to 610 nm and are named after common fruits that bear colors similar to their emission profiles.

Among the best red members in the Fruit series are mStrawberry and mCherry (Table 1; Fig. 3K; emission peaks at 596 nm and 610 nm), which have brightness levels of ~75% and 50% of EGFP, respectively. However, mCherry is far more photostable than mStrawberry and is the best choice to replace mRFP1 for long-term imaging experiments. These mFruits together with mKO and TagRFP, essentially fill the gap between the most red-shifted jellyfish FPs (such as YPet) and the multitude of oligomeric red coral FPs that have been reported and are now commercially available. Although several mFruits lack the brightness and photostability

necessary for many imaging experiments (Shaner et al., 2005; Tsien, 2005), their existence suggests that bright, stable, monomeric probes across the entire visible spectrum should eventually be available.

Further extension of the mFruit spectral class through a novel technique known as iterative somatic hypermutation (SMH) (Wang et al., 2004) has yielded two new FPs representing the first true far-red genetically engineered probes (emission wavelength maxima of 625 nm and 649 nm). The most potentially useful, mPlum (Fig. 3L), has rather limited brightness (10% of EGFP; Table 1) but excellent photostability. mPlum should be useful in combination with cyan, green, yellow and orange FPs for multicolor imaging experiments and as a FRET partner for green and yellow FPs, such as mEmerald (Förster distance 4.4) and mCitrine (Förster distance 5.0). Recently, several of the mFruit proteins have become commercially available (from Clontech).

Chudakov and associates (Shcherbo et al., 2007) have applied a combination of site-specific and random mutagenesis to generate libraries encoding TurboRFP variants that contain mutations at key positions surrounding the chromophore. After screening for mutants exhibiting far-red fluorescence and conducting additional rounds of random mutagenesis, they obtained a dimeric protein named Katushka (emission maximum of 635 nm; available from Evrogen as TurboFP635). Although only two-thirds as bright as EGFP, Katushka exhibits the highest brightness levels of any FP in the spectral window encompassing 650-800 nm, a region that is important for deep-tissue imaging. Introduction of the four principal Katushka mutations into TagRFP generated a monomeric, far-red protein named mKate (see Table 1; Evrogen, TagFP635) that has similar spectral characteristics. The photostability of mKate is reported to be exceptional and the protein displays brightness similar to that of mCherry, which makes it an excellent candidate for localization experiments in the far-red portion of the spectrum.

Increasing FP Stokes shift
In addition to engineering efforts designed to modulate the emission spectra, FP mutagenesis has also targeted the separation distance between absorption and emission maxima (Stokes shift) to generate better probes for FRET, fluorescence cross-correlation spectroscopy (FCCS) and multicolor imaging. Introducing the T203I mutation into wtGFP produces a variant, Sapphire, devoid of the minor excitation peak at 475 nm (Tsien, 1998). Sapphire exhibits a dramatic Stokes shift of 112 nm, having excitation and emission maxima at 399 nm and 511 nm, respectively. A derivative that displays improved folding and brighter fluorescence, T-Sapphire (T for Turbo), has four additional mutations (Zapata-Hommer and Griesbeck, 2003). These variants should be excellent donors in FRET combinations with orange and red proteins because of their ability to be excited in the ultraviolet region.

Extending the Sapphire strategy to red FPs, Miyawaki and associates (Kogure et al., 2006) used a far more rigorous approach to construct the longest Stokes shift FP variant yet developed (180 nm) using a chromoprotein derived from the *Montipora* stony coral. Semi-random mutagenesis of five residues surrounding the chromophore led to a red FP that has a bimodal excitation spectrum (peaks at 452 nm and 580 nm) with emission at 606 nm. An additional four mutations

substantially reduce the 580 nm peak and blue-shifted the other absorption peak to 440 nm. This derivative, named Keima (after the Japanese chess piece), exhibits an emission maximum at 616 nm, but is tetrameric. Several more rounds of mutagenesis produced a dimer (dKeima) that has similar spectral properties, and a monomer (mKeima; emission maximum = 620 nm). mKeima exhibits limited brightness (similar to that of mPlum) and requires a specialized filter combination for imaging, but it is useful in FCCS and multicolor imaging experiments (Kogure et al., 2006).

Although promising candidates are now available in every FP spectral class (see Fig. 3 and Table 1), in most cases there remains no EGFP equivalent, in terms of photostability and other crucial areas of performance (with the exception of pH stability). New additions to the blue and cyan region feature substantially improved brightness and photostability, and any of the orange FPs are excellent choices for long-term multicolor imaging. In addition, although brighter than EGFP, the YFPs still have suboptimal photostability, whereas the red and far-red FPs are among the dimmest in all spectral classes. Further compounding the problem is the potential for aggregation artifacts due to poorly folding proteins, regardless of the spectral class or supposedly monomeric characteristics (Kremers et al., 2007). Even so, many of the FPs listed in Table 1 can be combined for dual- and triple-color imaging to yield excellent results. Given that most of these proteins have only been introduced in the past couple of years, we remain optimistic that in the future, bright and photostable additions will become available for all spectral classes.

Advances in FP engineering
All of the FPs discovered thus far adopt a similar 3D cylindrical structure, in which a large portion of the polypeptide backbone is wound into 11 strands of an extensively hydrogen-bonded β-sheet that surround a central α-helix containing the chromophore, with short helical segments protecting the ends of the cylinder (Fig. 1) (Ormö et al., 1996; Remington, 2006; Yarbrough et al., 2001). The β-sheets are linked together by less-ordered proline-rich loops and the amino acid side chains in each sheet alternately project into the protein interior or towards the surface. Similar to most soluble proteins, the exterior residues are usually charged or polar, although there are also patches containing hydrophobic residues. The interior of the protein is so tightly packed that even water molecules are fixed into place by hydrogen bonds to the amino acids and there is little room for diffusion of ions or other intruding small molecules.

The rigidly defined structure of the FP interior is responsible for the unique chemical environment that nurtures autocatalytic chromophore formation by three of the amino acids in the central α-helix. Changes in this environment give rise to variations in spectral characteristics, photostability and many other physical properties. This concept is perhaps best exemplified by the fact that the common tripeptide Met-Tyr-Gly (MYG) is able to form chromophores spanning an astonishing 175-nm emission range, which is apparently dependent solely upon the nature of the chemical and physical environment provided by the interior of the β-barrel. Notable FPs featuring the MYG chromophore include ZsGreen1 (Clontech; emission maximum = 507), tdTomato (Shaner et al., 2004), TagRFP (Merzlyak et al., 2007), mCherry (Shaner et al.,

2004), mKate (Shcherbo et al., 2007), and mPlum (Wang et al., 2004). At the ends of the MYG spectral range are the cyan FP, AmCyan1 (Clontech; emission maximum = 486 nm), and the far-red FP, AQ14 (Shkrob et al., 2005) (emission maximum = 663 nm). Although the chromophore structures have yet to be elucidated for most of the reported FPs harboring the MYG triplet, they are likely to exhibit a wide range of diversity.

The first attempts to engineer new FPs logically targeted residues participating in the chromophore, as well as those in its immediate vicinity (Fig. 1). These efforts generated a variety of spectral variants that have emission profiles shifted by tens of nanometers to both lower and higher wavelengths. As crystal structures of the *Aequorea* FPs became available, protein engineers were able to rationally design new variants that feature an even wider range of mutations affecting spectral properties, photostability, oligomerization, pH sensitivity and maturation rates. The discovery of red-shifted FPs in corals similarly led to new variants that have an emission spectral range of ~160 nm and feature a high degree of variety in their properties. However, there are limits to the logical deductions that can be made from crystal structures and many of the variants generated through random mutagenesis suffer from reduced intensity and folding problems or lack fluorescence altogether. All too often, seemingly obvious mutations to alter a specific feature must be followed by one or more rounds of random mutagenesis to rescue other desirable properties. For these reasons, several groups have used innovative techniques to improve design strategies.

A promising approach that should be useful to fine-tune the properties of virtually any FP involves the coupling of a structure-based library in which specific residues are targeted with quantitative screening for improved or otherwise modified characteristics (Neylon, 2004; Park et al., 2004). This methodology was successfully applied to BFP in an attempt to enhance its brightness and photostability (Mena et al., 2006) by repacking the protein core with bulkier amino acid residues intended to constrain chromophore motions that reduce fluorescence emission through internal conversion mechanisms. The best variant exhibited an intrinsic brightness 60% greater than native BFP and was named Azurite, after the similarly colored mineral. Ironically, one of the two most beneficial mutations in this study occurred through the unintended incorporation of a new codon that alters position 224, which was not part of the design criteria. This finding highlights at least one potential limitation of the targeted library approach, but this does not outweigh the benefits that arise from reducing the number of experimental iteration cycles and thus the speed with which good candidates can be identified. It will be interesting to see whether the approach can be successfully applied to other FP properties.

Nguyen and Daugherty have employed a similar approach, termed evolutionary optimization, to optimize CFP and YFP when combined in a FRET biosensor equipped with a caspase-3 cleavage site to detect apoptosis (Nguyen and Daugherty, 2005). Hampered by the difficulty of using rational design to improve FRET performance, they used random mutagenesis to identify residues directly influencing FRET efficiency and then subjected these to partial or complete saturation mutagenesis through synthetic shuffling. The final result was YPet (see above) and a cyan variant, CyPet, that exhibits superior pH stability and faster maturation than ECFP. However, CyPet folds very poorly at 37°C, which severely limits its use as a stand-alone probe. Amino acid substitutions in CyPet and YPet are distributed throughout the proteins, beneficial mutations occurring both near and far away from the chromophore (Fig. 1). The CyPet-YPet FRET caspase-3 biosensor exhibits a 20-fold improvement in dynamic range over a similar mCerulean-mVenus pair. This impressive increase in efficiency has recently been challenged (Ohashi et al., 2007; Vinkenborg et al., 2007) by demonstrations that CyPet-YPet biosensors are prone to enhanced dimerization, which is largely responsible for their superior performance. Thus, careful consideration to this artifact should be given in the design of experiments using the CyPet-YPet combination.

The construction of new FP variants using guided consensus sequence engineering has been applied (Dai et al., 2007) to a monomeric green variant, Azami Green (mAG), derived from the stony coral genus *Galaxeidae* (Karasawa et al., 2003). Consensus engineering attempts to alter protein properties by modifying the sequence to one that more closely resembles a consensus derived from a large population of similar proteins in a particular family. The result, CGP (for consensus green protein), differs from mAG by 23 residues and by 76 residues from the most distant relative used to create the consensus (GFP2 from the coral *Agaricia fragilis*). CGP exhibits a high level of fluorescence when expressed in bacteria and is monomeric, but the quantum yield is reduced by almost 40% relative to mAG, rendering CGP significantly less bright. Interestingly, over 85% of the residues that differ from mAG to CGP are predicted to be found on the surface of the protein, probably reflecting the observation that surface residues evolve more quickly than internal residues. Although the first attempt at FP consensus engineering resulted in a product that is less efficient than the guide protein, this approach will undoubtedly become more useful as the database of known FP sequences grows.

The generation of GFP derivatives that have improved folding efficiencies when participating in fusion proteins was the basis for the work that produced superfolder GFP (Pédelacq et al., 2006) (see above). This variant was engineered by fusing libraries of shuffled GFP sequences to polypeptides that, by themselves, exhibit poor folding. The poorly folding peptides are termed bait proteins and interfere with the correct folding of the GFP moiety when expressed in bacteria. Pédelacq and colleagues started with a derivative consisting of cycle-3 GFP (also known as 'folding reporter' GFP) (Crameri et al., 1996), and the F64L and S65T mutations from EGFP (Patterson et al., 1997). After four rounds of DNA shuffling, the investigators isolated a brightly fluorescent clone that contains six new mutations in addition to the enhanced GFP and folding reporter mutations. The crucial point of the superfolder work is that there is yet more room for engineering improvements even in the highly optimized GFP derivatives. This approach, when applied to proteins from coral species in other color classes, may yield similar results.

A truly unique approach to genetic engineering of new FPs, pioneered by Roger Tsien and associates, involves directed evolution using a technique borrowed from the immune system, iterative somatic hypermutation (SHM) (Wang et al., 2004). They wanted to generate red FP derivatives that feature emission wavelengths in the far-red region (>625 nm). Noting that B lymphocytes can introduce point mutations into the

variable domains of antibodies through SHM, Wang and co-workers demonstrated that this technique could also be used to generate new phenotypes in FPs when expressed in a human B-cell line (Ramos) that hypermutates immunoglobulins. A derivative of mRFP1 under the control of a tetracycline-inducible promoter was expressed from a retroviral vector in the Ramos cell line and transcription was modulated by doxycycline to control the level of SHM, which preferentially targets highly transcribed genes. The resulting mutants were enriched by FACS to select clones exhibiting the longest emission wavelengths, and the process was repeated iteratively. After 23 rounds, a monomeric far-red-emitting protein named mPlum (see Table 1) was isolated and characterized. The mPlum emission spectrum maximum (649 nm) is shifted by 37 nm relative to the parent, and the FP also exhibits an unusually large Stokes shift of 59 nm. A second clone from an earlier SHM round, mRaspberry, has a shorter wavelength emission maximum (625 nm). Although mRaspberry is not photostable enough for applications in routine live-cell imaging, mPlum stability is comparable to that of many proteins in the yellow spectral class.

Fine-tuning existing proteins by improving their folding, brightness, oligomerization and photostability through the approaches described above will no doubt ultimately yield better probes than simply scouring the oceans for new candidates, which typically possess a common set of problems. The recent burst of activity in the development of FP engineering technology has led to several new variants that probably would not have been discovered by traditional methodology. These advanced techniques have been used to generate new colors, establish greater structural stability, enhance folding and optimize FRET efficiency. Perhaps new selection methods will enable the improvement of pH sensitivity and photostability, two areas that are crucial to high performance in acidic organelles and for long-term imaging experiments. Given that many of the amino acid triplets so far uncovered in chromophores can give rise to huge variations in emission color (e.g. MYG, 177 nm; QYG, 137 nm; TYG, 91 nm; CYG, 80 nm), it appears that there is plenty of room in the FP sequence space for additional mutations that will optimize color and many, if not all, of the other FP properties.

Optical highlighter FPs

Investigations into the complex photophysical properties of FP variants have led to the generation of chromophores that can be activated either to initiate fluorescence emission from a quiescent state (photoactivation) or to be optically converted from one fluorescence emission bandwidth to another (photoconversion). These proteins are emerging as a powerful new class of probes, ideal for investigation of protein dynamics in live-cell imaging (reviewed in Lippincott-Schwartz et al., 2003; Lukyanov et al., 2005; Remington, 2006). Perhaps more appropriately termed molecular or optical highlighters, photoactivatable or photoconvertible FPs can be used in the direct and controlled highlighting of distinct molecular pools within the cell. Because only a limited population of photoactivated molecules exhibits noticeable fluorescence, their lifetime and behavior can be followed independently. Ideal optical highlighters (see Table 2) should be readily photoactivatable/photoconvertable to generate a high level of contrast, and should be monomeric for optimal performance as

Table 2. Physical properties of useful optical highlighter fluorescent proteins

Protein*	Color of spectral class	Excitation peak (nm)	Emission peak (nm)	Brightness[†]	pKa[‡]	Association state[‡]	Chromophore	Filter set[§]	Reference
PA-GFP (N)[¶]	Green	400	515	2.7	4.5	Weak dimer	SYG	DAPI/FITC	Patterson and Lippincott-Schwartz, 2002
PA-GFP (P)**	Green	504	517	13.8	4.5	Weak dimer	SYG	FITC/GFP	Patterson and Lippincott-Schwartz, 2002
PS-CFP2 (N)	Cyan	400	468	8.6	4.3	Monomer	SYG	CFP	Chudakov et al., 2004
PS-CFP2 (P)	Green	490	511	10.8	6.1	Monomer	SYG	FITC/GFP	Chudakov et al., 2004
PA-mRFP1 (P)	Red	578	605	0.8	4.4	Monomer	QYG	TxRed	Verkhusha and Sorkin, 2005
tdEos (N)	Green	506	516	55.4	5.5	Tandem dimer	HYG	FITC/GFP	Nienhaus et al., 2006
tdEos (P)	Red	569	581	19.8	5.5	Tandem dimer	HYG	TRITC	Nienhaus et al., 2006
Dendra2 (N)	Green	490	507	22.5	6.6	Monomer	HYG	FITC/GFP	Gurskaya et al., 2006
Dendra2 (P)	Red	553	573	19.3	6.9	Monomer	HYG	TRITC	Gurskaya et al., 2006
KFP1 (P)	Red	580	600	4.1	NA	Tetramer	MYG	TRITC/DsRed	Labas et al., 2002
Dronpa (P)	Green	503	518	80.8	5.0	Monomer	CYG	FITC/GFP	Ando et al., 2004

Table of physical properties for the monomeric and tandem dimer optical highlighters. *Common literature FP abbreviation. [†]Product of the molar extinction coefficient and the quantum yield (mM×cm)$^{-1}$. [‡]Literature values except as noted. [§]Recommended common filter sets and custom FP sets available from aftermarket manufacturers. For specialized applications, we suggest choosing filter combinations that closely match the spectral profiles (see Shaner et al., 2005). [¶]Native conformation. **Photoactivated or photoconverted conformation.

fusion tags. They offer a gentler alternative to the relatively harsh photobleaching techniques, such as fluorescence recovery after photobleaching (FRAP) and fluorescence loss in photobleaching (FLIP), which generally require high laser powers and repeated illumination to completely eradicate active fluorophores from the region of interest. Furthermore, measurements are not negatively influenced by freshly synthesized or non-converted FPs, which either remain invisible or continue to emit the original wavelengths.

The first photoactivatable (PA) optical highlighter PA-GFP (Fig. 4A and Table 2), was derived from wtGFP by the substitution of histidine for threonine at position 203 (T203H) to produce a variant devoid of green fluorescence until activated (Patterson and Lippincott-Schwartz, 2002). Irradiation with intense violet light (390-415 nm) produces a 100-fold increase in green fluorescence (emission peak at 504 nm), enabling tracking of the dynamics in molecular subpopulations (Fig. 5A-C). PA-GFP is difficult to detect in its non-activated form, which is perhaps the greatest pitfall in determining regions for examination. However, this feature is crucial for establishing a high dynamic range for photoactivation. Similar FPs based on Emerald and superfolder GFP display a reduced dynamic range (M.W.D., unpublished), probably because the non-activated state is significantly brighter than that of PA-GFP.

A new protein derived from the jellyfish *Aequorea coerulescens*, photoswitchable (PS)-CFP2, photoconverts from cyan to green fluorescence upon illumination at 405 nm (Table 2). This optical highlighter features the same chromophore as

PA-GFP (SYG) and may be photoactivated through a similar mechanism (Fig. 4A). PS-CFP2 has an advantage over PA-GFP in that a significant level of cyan fluorescence is present before photoconversion, which enables easier tracking and determination of regions for selective illumination. However, the dynamic range of PS-CFP2 is lower than that of PA-GFP and the probe is inferior to green-to-red optical highlighters in terms of photoconversion efficiency.

All of the green-to-red optical highlighters so far reported (including Dendra2, Eos, Kaede, and KikGR, Table 2) contain a chromophore derived from the tripeptide His-Tyr-Gly (HYG) that initially emits green fluorescence. Irradiation with short wavelength visible or long wavelength ultraviolet light induces cleavage between the amide nitrogen and α-carbon atoms in the histidine residue with subsequent extension of chromophore conjugation to the histidine side chain (Fig. 4B). This process requires catalysis by the intact protein and results in a dramatic shift of fluorescence emission to longer (orange-red) wavelengths (Mizuno et al., 2003; Nienhaus et al., 2005). The unconventional chemistry involved in this chromophore transition provides an excellent foundation upon which to develop more advanced highlighters.

Unfortunately, the full potential for optical highlighters is yet to be realized. Of the few photoactivatable probes available, PA-GFP is still the best choice in the green region of the palette and is far superior in terms of dynamic range to the only red variant yet reported, PA-mRFP1 (Verkhusha and Sorkin, 2005). The only choice for cyan-to-green photoconversion, PS-CFP2 (Chudakov et al., 2004), exhibits
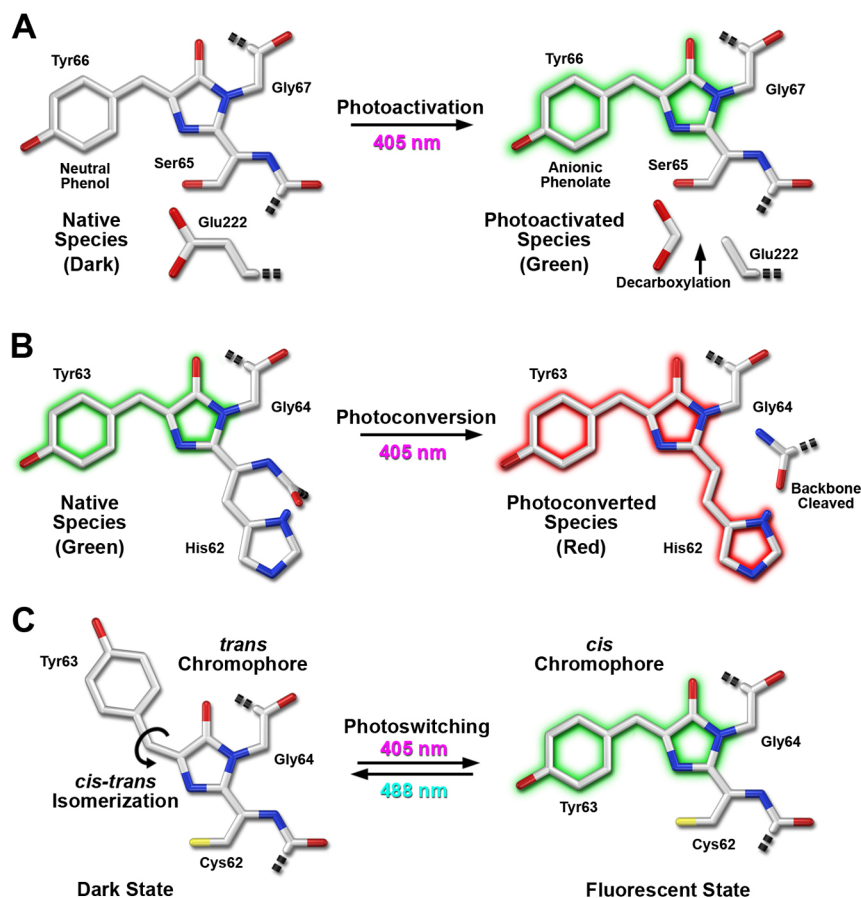

Fig. 4. Photoactivation, photoconversion and photoswitching mechanisms for optical highlighter FPs. (A) Photoactivation of PA-GFP (illustrated) and PS-CFP2 is believed to occur due to decarboxylation of Glu222 followed by conversion of the chromophore from a neutral to anionic state. (B) Green-to-red photoconversion for Kaede, KikGR, Dendra2 and Eos, all of which contain the HYG chromophore, occurs when the FP is illuminated with ultraviolet or violet radiation to induce cleavage between the amide nitrogen and α-carbon atoms in the His62 residue leading to subsequent formation of a conjugated dual imidazole ring system. (C) Photoswitching of Dronpa involves cis-trans photoisomerization induced by alternating radiation between 405 nm and 488 nm. A similar isomerization mechanism is suggested to operate in mTFP0.7 and KFP1.

monomeric character but is hampered by low brightness levels and the artifact of continued photoconversion during imaging. In the green-to-red class, the best performers in terms of brightness and conversion efficiency are Kaede and KikGR (Ando et al., 2002; Tsutsui et al., 2005). However, both are tetrameric and thus not useful for most experiments. A monomeric variant, Dendra2 (Gurskaya et al., 2006), is probably the best choice for sensitive fusions and FRET studies (see Fig. 5G-I), but suffers from rapid photobleaching of the red species during laser scanning confocal imaging and is <50% as bright as the tetramers. The tandem dimer of the green-to-red highlighter named Eos (Nienhaus et al., 2006; Wiedenmann et al., 2004) is better than Dendra2 in terms of brightness and photostability but twice as large (see Fig. 5D-F). Clearly, there is need for better performers in all categories.

A new generation of specialized reversible optical highlighters with on-off switching capabilities was heralded by the introduction of Dronpa, a monomeric FP derived from Pectiniidae (Ando et al., 2004; Habuchi et al., 2005). Dronpa, which was engineered by directed and random mutagenesis, exhibits unusual photochromic behavior characterized by its ability to toggle fluorescence on and off following illumination with two different excitation wavelengths (Fig. 4C and Fig. 5J-L). Dronpa has an absorption maximum at 503 nm with a minor peak at 390 nm. The major peak is due to the deprotonated (anionic) species of the chromophore, whereas

the minor peak arises from the protonated (neutral) form. When irradiated at 488 nm, the anionic species emits at a maximum of 518 nm with a relatively high quantum yield of 0.85 (Table 2). By contrast, the neutral form of the chromophore is almost non-fluorescent. Photoswitching of Dronpa occurs by interconversion between the deprotonated and protonated forms (Habuchi et al., 2005). Upon irradiation at 488 nm, Dronpa is driven to the protonated species with a commitment decrease in fluorescence to produce a dim (off) state in which the 390-nm absorption peak predominates. The dim state is readily converted back to the original fluorescent (on) deprotonated state with minimal illumination at 405 nm (Fig. 4C). Similar behavior has been reported for a teal FP precursor, termed mTFP0.7 (Henderson et al., 2007), in which the dark and fluorescent states have been characterized by crystallography.

Another photoswitchable highlighter, Kindling FP (commercially available from Evrogen as KFP1; Table 2), has been developed from a non-fluorescent chromoprotein isolated from *Anemonia sulcata* (Chudakov et al., 2003a). KFP1 does not exhibit fluorescence emission until illuminated with green or yellow light in the region between 525 nm and 580 nm. Low-intensity light results in transient red fluorescence (termed kindling) that has excitation and emission maxima at 580 nm and 600 nm, respectively, which slowly decays upon cessation of illumination as the protein relaxes back to its
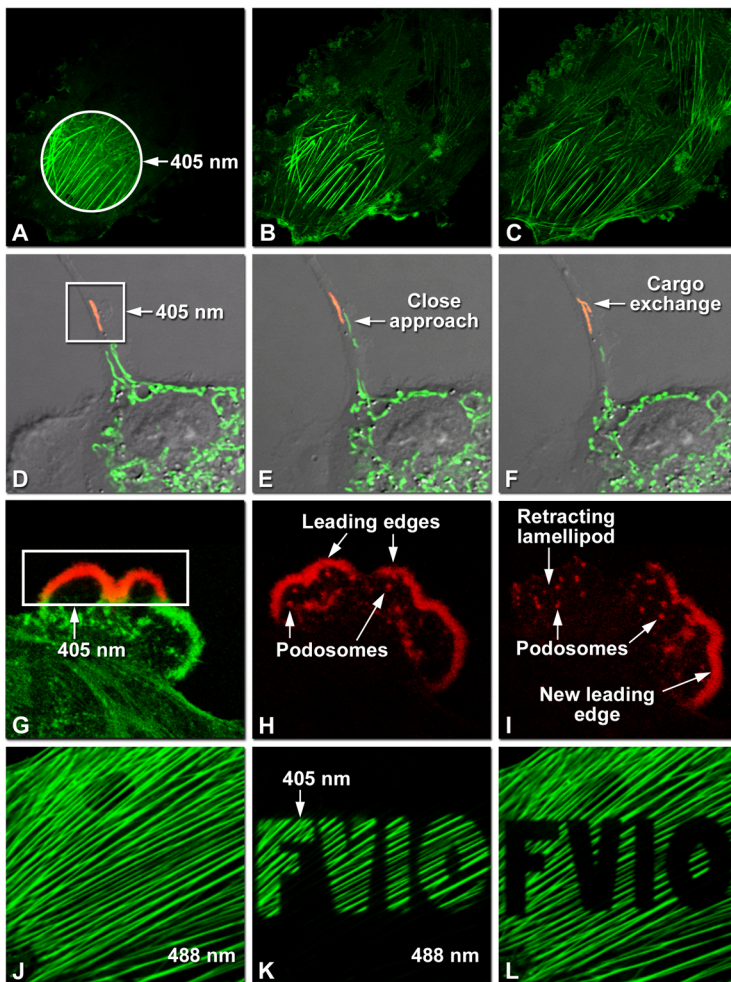

Fig. 5. Optical highlighter FPs in action imaged with laser scanning confocal microscopy. (A-C) Photoactivation of mPA-GFP-actin-C-7 in opossum kidney (OK cell line) epithelial cells. (A) Circular region of interest selected with an Olympus FV1000 tornado scanner is illuminated at 405 nm for 5 seconds, *t*=0 minutes. (B) The photoactivated actin chimera first translocates to the ruffles at the cellular margins as fluorescence intensity decreases in the activated region, *t*=5 minutes. (C) Ruffles, cytoplasmic actin pools and the filamentous actin network gain more intensity at *t*=60 minutes. (D-F) Tracking of mitochondria labeled with tdEos-mito-N-7 in rabbit kidney (RK-13 cell line) epithelial cells. (D) Photoconversion of a single mitochondrion (red) in a selected region at 405 nm illumination, *t*=0 minutes. (E) Close approach of a non-converted (green) mitochondrion (arrow), *t*=10 minutes. (F) Cargo exchange between mitochondria (arrow), *t*=20 minutes. (G-I) Examination of lamellipodia with Dendra2-actin-C-7 in OK cells. (G) Photoconversion (red) of the selected region (box) with a 405 nm laser, *t*=0 minutes. (H) The photoconverted channel illustrates podosome formation by photoconverted actin and changes in leading edges, *t*=20 minutes. (I) Photoconverted lamellipod retracts amid increased podosome formation and generation of a new leading edge, *t*=45 minutes. (J-L) Photoswitching of the actin cytoskeleton with Dronpa-actin-C-7 in rat thoracic aorta (A7r5 cell line) myoblasts. (J) Actin network imaged with a 488-nm laser, *t*=0 minutes. (K) After completely photoswitching the labeled actin 'off' at 488 nm, the region spelling FV10 was activated with a 405 nm laser, *t*=3 minutes. (L) FV10 region photobleached while imaging the actin network at 488 nm.
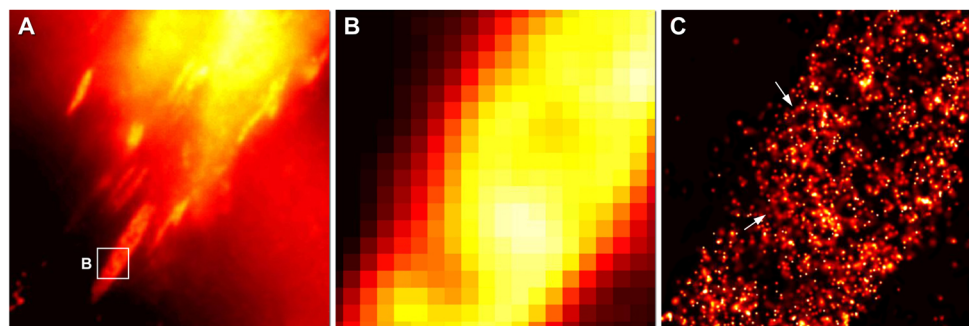
Fig. 6. Photoactivated localization microscopy (PALM) imaging of focal adhesions near the coverslip surface in paraformaldehyde-fixed Gray fox lung fibroblast cells. (A) Widefield fluorescence image of multiple focal adhesions labeled with tdEos fused to human vinculin. (B) Total internal reflection fluorescence (TIRF) summed-molecule image of the focal adhesion within the region indicated by the box in A. (C) PALM view of the focal adhesion structure shown in B, which includes the apparent assembly of vinculin into a partial network (arrows).

initial non-fluorescent state. Irradiation with intense blue light (450-490 nm) completely quenches the red fluorescence immediately, allowing tight control over fluorescent labeling. By contrast, high-intensity green illumination (~550 nm) or continued irradiation at moderate levels results in irreversible photoconversion to give a fluorescence intensity ~30-fold greater than that of the non-activated protein. The major drawback of KFP1 is its obligatory tetramerization, which seriously affects its potential for use as a fusion tag or FRET partner.

Investigations into the mechanism of FP photoswitching (Andresen et al., 2005; Andresen et al., 2007; Chudakov et al., 2003b; Henderson et al., 2007; Stiel et al., 2007) suggest that cis-trans isomerization of the hydroxybenzilidine chromophore moiety is a key event in the switching process. The cis conformation represents the fluorescent state, whereas the trans isomer is adopted by the chromophore in the non-fluorescent, or dark, state (Fig. 4C). These conformational changes are apparently accompanied by varied protonation states of the chromophore that help determine the fluorescent properties (as discussed above). Furthermore, light-induced photoswitching is probably a manifestation of chromophore planarity and structural rearrangements of internal amino acid side chains within the chromophore cavity. These collective features may constitute a fundamental mechanism that is common to all photoactivatable and reversibly photoswitchable FP derivatives.

In addition to their use for selectively labeling subpopulations of fusion proteins for dynamic studies, optical highlighters are also valuable tools in superresolution microscopy techniques designed to break the traditional Abbe diffraction barrier (Betzig et al., 2006; Egner et al., 2007; Hell, 2007; Hess et al., 2006). Newly introduced methods such as photoactivated localization microscopy (PALM; Fig. 6) and stochastic optical reconstruction microscopy (STORM) rely on low levels of illumination to photoactivate selected individual molecules spaced further apart than the diffraction limit so that an array of magnified diffraction spots can be recorded on a highly sensitive camera. Adjacent molecules are not recorded because they still exist in the dark or inactivated state. Calculation of the exact coordinates of the single fluorescent molecules within the photoactivated population enables precise localization. Finally, after switching off (or

photobleaching) the registered molecules, a new group can be photoactivated and read out. Thus, the image is assembled one molecule at a time by means of iterative switching cycles. The reconstructed images feature optical resolutions down to 10 nm. These techniques are becoming increasingly fast and hold significant promise for live cell imaging at unprecedented resolution.

The unique photoactivation probes, green-to-red optical highlighters, and photoswitchable variants produced thus far from GFP derivatives and reef coral proteins certainly warrant aggressive efforts to solve the problems associated with aggregation and fine-tune their photoactivation requirements and emission profiles. In the future, the engineering of advanced optical highlighter proteins that shift photoconversion illumination wavelengths to the blue and green spectral regions (which are significantly less toxic to living cells than the ultraviolet wavelengths currently required), as well as shifting emission wavelengths to the yellow through the far-red region, will greatly expand the potential applications for this class of probes.

Conclusions

Continuing efforts in protein engineering of the existing FPs, coupled with advanced new screening technologies, should further expand the available color palette and ultimately provide rapidly maturing, bright, and photostable proteins in every spectral class. As the development of optical highlighters continues, FPs useful for optical marking should evolve towards brighter, monomeric derivatives that exhibit high contrast and can be easily photoconverted to display a wide spectrum of emission colors. Proteins capable of reversible photoactivation, red-to-green photoconversion, improved expression at elevated temperatures, and derivatives emitting in the far-red or near-infrared regions of the spectrum would be especially useful.

References

Ai, H., Henderson, J. N., Remington, S. J. and Campbell, R. E. (2006). Directed evolution of a monomeric, bright and photostable version of *Clavularia* cyan fluorescent protein: structural characterization and applications in fluorescence imaging. *Biochem. J.* **400**, 531-540.

Ai, H., Shaner, N. C., Cheng, Z., Tsien, R. Y. and Campbell, R. E. (2007). Exploration of new chromophore structures leads to the identification of improved blue fluorescent proteins. *Biochemistry* **46**, 5904-5910.

Ando, R., Hama, H., Yamamoto-Hino, M., Mizuno, H. and Miyawaki, A. (2002). An optical marker based on the UV-induced green-to-red-photoconversion of a fluorescent protein. *Proc. Natl. Acad. Sci. USA* **99**, 12651-12656.

Ando, R., Mizuno, H. and Miyawaki, A. (2004). Regulated fast nucleocytoplasmic shuttling observed by reversible protein highlighting. *Science* **306**, 1370-1373.

Andresen, M., Wahl, M. C., Stiel, A. C., Gräter, F., Schäfer, L. V., Trowitzsch, S., Weber, G., Eggeling, C., Grubmüller, H., Hell, S. W. et al. (2005). Structure and mechanism of the reversible photoswitch of a fluorescent protein. *Proc. Natl. Acad. Sci. USA* **102**, 13070-13074.

Andresen, M., Stiel, A. C., Trowitzsch, S., Weber, G., Eggeling, C., Wahl, M. C., Hell, S. W. and Jakobs, S. (2007). Structural basis for reversible photoswitching in Dronpa. *Proc. Natl. Acad. Sci. USA* **104**, 13005-13009.

Betzig, E., Patterson, G. H., Sougrat, R., Lindwasser, O. W., Olenych, S., Bonifacino, J. S., Davidson, M. W., Lippincott-Schwartz, J. and Hess, H. F. (2006). Imaging intracellular fluorescent proteins at nanometer resolution. *Science* **313**, 1642-1645.

Campbell, R. E., Tour, O., Palmer, A. E., Steinbach, P. A., Baird, G. S., Zacharias, D. A. and Tsien, R. Y. (2002). A monomeric red fluorescent protein. *Proc. Natl. Acad. Sci. USA* **99**, 7877-7882.

Chalfie, M., Tu, Y., Euskirchen, G., Ward, W. W. and Prasher, D. C. (1994). Green fluorescent protein as a marker for gene expression. *Science* **263**, 802-805.

Chudakov, D. M., Belousov, V. V., Zaraisky, A. G., Novoselov, V. V., Staroverov, D. B., Zorov, D. B., Lukyanov, S. and Lukyanov, K. A. (2003a). Kindling fluorescent proteins for precise *in vivo* photolabeling. *Nat. Biotechnol.* **21**, 191-194.

Chudakov, D. M., Feofanov, A. V., Mudrik, N. N., Lukyanov, S. and Lukyanov, K. A. (2003b). Chromophore environment provides clue to "kindling fluorescent protein" riddle. *J. Biol. Chem.* **278**, 7215-7219.

Chudakov, D. M., Verkhusha, V. V., Staroverov, D. B., Souslova, E. A., Lukyanov, S. and Lukyanov, K. A. (2004). Photoswitchable cyan fluorescent protein for protein tracking. *Nat. Biotechnol.* **22**, 1435-1439.

Chudakov, D. M., Lukyanov, S. and Lukyanov, K. A. (2005). Fluorescent proteins as a toolkit for *in vivo* imaging. *Trends Biotechnol.* **23**, 605-613.

Crameri, A., Whitehorn, E. A., Tate, E. and Stemmer, W. P. (1996). Improved green fluorescent protein by molecular evolution using DNA shuffling. *Nat. Biotechnol.* **14**, 315-319.

Cubitt, A. B., Heim, R., Adams, S. R., Boyd, A. E., Gross, L. A. and Tsien, R. Y. (1995). Understanding, improving and using green fluorescent proteins. *Trends Biochem. Sci.* **20**, 448-455.

Cubitt, A. B., Woolenweber, L. A. and Heim, R. (1999). Understanding structure-function relationships in the *Aequorea victoria* green fluorescent protein. *Methods Cell Biol.* **58**, 19-30.

Dai, M., Fisher, H. E., Temirov, J., Kiss, C., Phipps, M. E., Pavlik, P., Werner, J. H. and Bradbury, A. R. M. (2007). The creation of a novel fluorescent protein by guided consensus engineering. *Protein Eng. Des. Sel.* **20**, 69-79.

Deheyn, D. D., Kubokawa, K., McCarthy, J. K., Murakami, A., Porrachia, M., Rouse, G. W. and Holland, N. D. (2007). Endogenous green fluorescent protein (GFP) in amphioxus. *Biol. Bull.* **213**, 95-100.

Egner, A., Geisler, C., von Middendorff, C., Bock, H., Wenzel, D., Medda, R., Andresen, M., Stiel, A. C., Jakobs, S., Eggeling, C. et al. (2007). Fluorescence nanoscopy in whole cells by asynchronous localization of photoswitching emitters. *Biophys. J.* **93**, 3285-3290.

Griesbeck, O., Baird, G. S., Campbell, R. E., Zacharias, D. A. and Tsien, R. Y. (2001). Reducing the environmental sensitivity of yellow fluorescent protein: Mechanism and applications. *J. Biol. Chem.* **276**, 29188-29194.

Gurskaya, N. G., Verkhusha, V. V., Shcheglov, A. S., Staroverov, D. M., Chepurnykh, T. V., Fradkov, A. F., Lukyanov, S. and Lukyanov, K. A. (2006). Engineering of a monomeric green-to-red photoactivatable fluorescent protein induced by blue light. *Nat. Biotechnol.* **24**, 461-465.

Habuchi, S., Ando, R., Dedecker, P., Verheijen, W., Mizuno, H., Miyawaki, A. and Hofkens, J. (2005). Reversible single-molecule photoswitching in the GFP-like fluorescent protein Dronpa. *Proc. Natl. Acad. Sci. USA* **102**, 9511-9516.

Heim, R. and Tsien, R. Y. (1996). Engineering green fluorescent protein for improved brightness, longer wavelengths and fluorescence resonance energy transfer. *Curr. Biol.* **6**, 178-182.

Heim, R., Prasher, D. C. and Tsien, R. Y. (1994). Wavelength mutations and post-translational autoxidation of green fluorescent protein. *Proc. Natl. Acad. Sci. USA* **91**, 12501-12504.

Heim, R., Cubitt, A. B. and Tsien, R. Y. (1995). Improved green fluorescence. *Nature* **373**, 663-664.

Hell, S. W. (2007). Far-field optical nanoscopy. *Science* **316**, 1153-1158.

Henderson, N. J., Ai, H.-W., Campbell, R. E. and Remington, S. J. (2007). Structural basis for reversible photobleaching of a green fluorescent protein homologue. *Proc. Natl. Acad. Sci. USA* **104**, 6672-6677.

Hess, S. T., Girirajan, T. P. K. and Mason, M. D. (2006). Ultra-high resolution imaging by fluorescence Photoactivation localization microscopy. *Biophys. J.* **91**, 4258-4272.

Karasawa, S., Araki, T., Yamamoto-Hino, M. and Miyawaki, A. (2003). A green-emitting fluorescent protein from *Galaxeidae* coral and its monomeric version for use in fluorescent labeling. *J. Biol. Chem.* **278**, 34167-34171.

Karasawa, S., Araki, T., Nagi, T., Mizuno, H. and Miyawaki, A. (2004). Cyan-emitting and orange-emitting fluorescent proteins as a donor/acceptor pair for fluorescence resonance energy transfer. *Biochem. J.* **381**, 307-312.

Kogure, T., Karasawa, S., Araki, T., Saito, K., Kinjo, M. and Miyawaki, A. (2006). A fluorescent variant of a protein from the stony coral *Montipora* facilitates dual-color single-laser fluorescence cross-correlation spectroscopy. *Nat. Biotechnol.* **24**, 577-581.

Kremers, G.-J., Goedhart, J., van Munster, E. B. and Gadella, T. W. J. (2006). Cyan and yellow super fluorescent proteins with improved brightness, protein folding, and FRET Förster radius. *Biochemistry* **45**, 6570-6579.

Kremers, G.-J., Goedhart, J., van den Heuvel, D. J., Gerritsen, H. C. and Gadella, T. W. J. (2007). Improved green and blue fluorescent proteins for expression in bacteria and mammalian cells. *Biochemistry* **46**, 3775-3783.

Labas, Y. A., Gurskaya, N. G., Yanushevich, Y. G., Fradkov, A. F., Lukyanov, K. A., Lukyanov, S. A. and Matz, M. V. (2002). Diversity and evolution of the green fluorescent protein family. *Proc. Natl. Acad. Sci. USA* **99**, 4256-4261.

Lippincott-Schwartz, J., Altan-Bonnet, N. and Patterson, G. H. (2003). Photobleaching and photoactivation: following protein dynamics in living cells. *Nat. Cell Biol.* **5**, S7-S14.

Lukyanov, K. A., Chudakov, D. M., Lukyanov, S. and Verkhusha, V. V. (2005). Innovation: photoactivatable fluorescent proteins. *Nat. Rev. Mol. Cell Biol.* **6**, 885-891.

Malo, G. D., Pouwels, L. J., Wang, M., Weichsel, A., Montfort, W. R., Rizzo, M. A., Piston, D. W. and Wachter, R. M. (2007). X-ray structure of Cerulean GFP: a tryptophan-based chromophore useful for fluorescence lifetime imaging. *Biochemistry* **46**, 9865-9873.

Matz, M. V., Fradkov, A. F., Labas, Y. A., Savitsky, A. P., Zaraisky, A. G., Markelov, M. L. and Lukyanov, S. A. (1999). Fluorescent proteins from nonbioluminescent Anthozoa species. *Nat. Biotechnol.* **17**, 969-973.

Mena, M. A., Treynor, T. P., Mayo, S. L. and Daugherty, P. S. (2006). Blue fluorescent proteins with enhanced bright brightness and photostability from a structurally targeted library. *Nat. Biotechnol.* **24**, 1569-1571.

Merzlyak, E. M., Goedhart, J., Shcherbo, D., Bulina, M. E., Shcheglov, A. S., Fradkov, A. F., Gaintzeva, A., Lukyanov, K. A., Lukyanov, S., Gadella, T. W. J. et al. (2007). Bright monomeric red fluorescent protein with an extended fluorescent lifetime. *Nat. Methods* **4**, 555-557.

Miyawaki, A., Griesbeck, O., Heim, R. and Tsien, R. Y. (1999). Dynamic and quantitative calcium measurements using improved cameleons. *Proc. Natl. Acad. Sci. USA* **96**, 2135-2140.

Mizuno, H., Mal, T. K., Tong, K. I., Ando, R., Furuta, T., Ikura, M. and Miyawaki, A. (2003). Photo-induced peptide cleavage in the green-to-red conversion of a fluorescent protein. *Mol. Cell* **12**, 1051-1058.

Nagai, T., Ibata, K., Park, E. S., Kubota, M., Mikoshiba, K. and Miyawaki, A. (2002). A variant of yellow fluorescent protein with fast and efficient maturation for cell-biological applications. *Nat. Biotechnol.* **20**, 87-90.

Neylon, C. (2004). Chemical and biochemical strategies for the randomization of protein encoding DNA sequences: library construction methods for directed evolution. *Nucleic Acids Res.* **32**, 1448-1459.

Nguyen, A. W. and Daugherty, P. S. (2005). Evolutionary optimization of fluorescent proteins for intracellular FRET. *Nat. Biotechnol.* **23**, 355-360.

Nienhaus, G. U., Nienhaus, K., Hölzle, A., Ivanchenko, S., Renzi, F., Oswald, F., Wolff, M., Schmitt, F., Röcker, E., Ballone, B. et al. (2006). Photoconvertible fluorescent protein EosFP: Biophysical properties and cell biology applications. *Photochem. Photobiol.* **82**, 351-358.

Nienhaus, K., Nienhaus, G. U., Wiedenmann, J. and Nar, H. (2005). Structural basis for photo-induced protein cleavage and green to red conversion of fluorescent protein EosFP. *Proc. Natl. Acad. Sci. USA* **102**, 9156-9159.

Ohashi, T., Galiacy, S. D., Briscoe, G. and Erickson, H. P. (2007). An experimental study of GFP-based FRET, with application to intrinsically unstructured proteins. *Protein Sci.* **16**, 1429-1438.

Olenych, S. G., Claxton, N. S., Ottenberg, G. K. and Davidson, M. W. (2006). The fluorescent protein color palette. *Curr. Protoc. Cell Biol.* 21.5.1-21.5.34.

Ormö, M., Cubitt, A. B., Kallio, K., Gross, L. A., Tsien, R. Y. and Remington, S. J. (1996). Crystal structure of the *Aequorea victoria* green fluorescent protein. *Science* **273**, 1392-1395.

Park, S., Yang, X. and Saven, J. G. (2004). Advances in computational protein design. *Curr. Opin. Struct. Biol.* **14**, 487-494.

Patterson, G. H. (2004). A new harvest of fluorescent proteins. *Nat. Biotechnol.* **22**, 1524-1525.

Patterson, G. H. (2007). Fluorescent proteins for cell biology. In *Reporter Genes: A Practical Guide* (ed. D. S. Anson), pp. 47-80. Totowa, NJ: Humana Press.

Patterson, G. H. and Lippincott-Schwartz, J. (2002). A photoactivatable GFP for selective photolabeling of proteins and cells. *Science* **297**, 1873-1877.

Patterson, G. H., Knobel, S. M., Sharif, W. D., Kain, S. R. and Piston, D. W. (1997). Use of the green fluorescent protein and its mutants in quantitative fluorescence microscopy. *Biophys. J.* **73**, 2782-2790.

Pédelacq, J.-D., Cabantous, S., Tran, T., Terwilliger, T. C. and Waldo, G. S. (2006). Engineering and characterization of a superfolder green fluorescent protein. *Nat. Biotechnol.* **24**, 79-88.

Petersen, J., Wilmann, P. G., Beddoe, T., Oakley, A. J., Devenish, R. J., Prescott, M. and Rossjohn, J. (2003). The 2.0 Å crystal structure of eqFP611, a far red fluorescent

protein from the sea anemone *Entacmaea quadricolor*. *J. Biol. Chem.* **278**, 44626-55631.

Remington, S. J. (2006). Fluorescent proteins: maturation, photochemistry and photophysics. *Curr. Opin. Struct. Biol.* **16**, 714-721.

Remington, S. J., Wachter, R. M., Yarbrough, D. K., Branchaud, B., Anderson, D. C., Kallio, K. and Lukyanov, K. A. (2005). zFP538, a yellow-fluorescent protein from Zoanthus, contains a novel three-ring chromophore. *Biochemistry* **44**, 202-212.

Rizzo, M. A. and Piston, D. W. (2005). Fluorescent protein tracking and detection. In *Live Cell Imaging: A Laboratory Manual* (ed. R. D. Goldman and D. L. Spector), pp. 3-23. Cold Spring Harbor: Cold Spring Harbor Laboratory Press.

Rizzo, M. A., Springer, G. H., Granada, B. and Piston, D. W. (2004). An improved cyan fluorescent protein variant useful for FRET. *Nat. Biotechnol.* **22**, 445-449.

Shcherbo, D., Merzlyak, E. M., Chepurnykh, T. V., Fradkov, A. F., Ermakova, G. V., Solovieva, E. A., Lukyanov, K. A., Bogdanova, E. A., Zaraisky, A. G., Lukyanov, S. et al. (2007). Bright far-red fluorescent protein for whole-body imaging. *Nat. Methods* **4**, 741-746.

Shagin, D. A., Barsova, E. V., Yanushevich, Y. G., Fradkov, A. F., Lukyanov, K. A., Labas, Y. A., Semenova, T. N., Ugalde, J. A., Meyers, A., Nunez, J. M. et al. (2004). GFP-like proteins as ubiquitous metazoan superfamily: Evolution of functional features and structural complexity. *Mol. Biol. Evol.* **21**, 841-850.

Shaner, N. C., Campbell, R. E., Steinbach, P. A., Giepmans, B. N. G., Palmer, A. E. and Tsien, R. Y. (2004). Improved monomeric red, orange and yellow fluorescent proteins derived from *Discosoma* sp. red fluorescent protein. *Nat. Biotechnol.* **22**, 1567-1572.

Shaner, N. C., Steinbach, P. A. and Tsien, R. Y. (2005). A guide to choosing fluorescent proteins. *Nat. Methods* **2**, 905-909.

Shkrob, M. A., Yanushevich, Y. G., Chudakov, D. M., Gurskaya, N. G., Labas, Y. A., Poponov, S. Y., Mudrik, N. N., Lukyanov, S. and Lukyanov, K. A. (2005). Far-red fluorescent proteins evolved from a blue chromoprotein from *Actinia equine*. *Biochem. J.* **392**, 649-654.

Shu, X., Shaner, N. C., Yarbrough, C. A., Tsien, R. Y. and Remington, S. J. (2006). Novel chromophores and buried charges control color in mFruits. *Biochemistry* **45**, 9639-9647.

Stiel, A. C., Trowitzsch, S., Weber, G., Andresen, M., Eggeling, C., Hell, S. W., Jakobs, S. and Wahl, M. C. (2007). 1.8 Å bright-state structure of the reversible switchable fluorescent protein Dronpa guides the generation of fast switching variants. *Biochem. J.* **402**, 35-42.

Tsien, R. Y. (1998). The green fluorescent protein. *Annu. Rev. Biochem.* **67**, 509-544.

Tsien, R. Y. (2005). Building and breeding molecules to spy on cells and tumors. *FEBS Lett.* **579**, 927-932.

Tsutsui, H., Karasawa, S., Shimizu, H., Nukina, N. and Miyawaki, A. (2005). Semi-rational engineering of a coral fluorescent protein into an efficient highlighter. *EMBO Rep.* **6**, 233-238.

Verkhusha, V. V. and Lukyanov, K. A. (2004). The molecular properties and applications of Anthozoa fluorescent proteins and chromoproteins. *Nat. Biotechnol.* **22**, 289-296.

Verkhusha, V. V. and Sorkin, A. (2005). Conversion of the monomeric red fluorescent protein into a photoactivatable probe. *Chem. Biol.* **12**, 279-285.

Vinkenborg, J. L., Evers, T. H., Reulen, S. W. A., Meijer, E. W. and Merkx, M. (2007). Enhanced sensitivity of FRET-based protease sensors by redesign of the GFP dimerization interface. *Chembiochem* **8**, 1119-1121.

Wang, L., Jackson, W. C., Steinbach, P. A. and Tsien, R. Y. (2004). Evolution of new nonantibody proteins via iterative somatic hypermutation. *Proc. Natl. Acad. Sci. USA* **101**, 16745-16749.

Wiedenmann, J., Ivanchenko, S., Oswald, F., Schmitt, F., Rocker, C., Salih, A., Spindler, K. and Nienhaus, G. U. (2004). EosFP, a fluorescent marker protein with UV-inducible green-to-red fluorescence conversion. *Proc. Natl. Acad. Sci. USA* **101**, 15905-15910.

Yarbrough, D., Wachter, R. M., Kallio, K., Matz, M. and Remington, S. J. (2001). Refined crystal structure of DsRed, a red fluorescent protein from coral, at 2.0-Å resolution. *Proc. Natl. Acad. Sci. USA* **98**, 462-467.

Zacharias, D. A., Violin, J. D., Newton, A. C. and Tsien, R. Y. (2002). Partitioning of lipid-modified monomeric GFPs into membrane microdomains of live cells. *Science* **296**, 913-916.

Zapata-Hommer, O. and Griesbeck, O. (2003). Efficiently folding and circularly permuted variants of the Sapphire mutant of GFP. *BMC Biotechnol.* **3**, 5-11.